Periplasmic Metal-Resistance Protein CusF Exhibits High Affinity and Specificity for Both Cu^I and Ag^I[†]

Joshua T. Kittleson,[‡] Isabell R. Loftin,[‡] Andrew C. Hausrath,[‡] Kevin P. Engelhardt,[‡] Christopher Rensing,[§] and Megan M. McEvoy*[‡]

Departments of Biochemistry and Molecular Biophysics, and Soil, Water, and Environmental Science, University of Arizona, Tucson, Arizona 85721

ABSTRACT: The periplasmic protein CusF, as a part of the CusCFBA efflux complex, plays a role in resistance to elevated levels of copper and silver in *Escherichia coli*. Although homologues have been identified in other Gram-negative bacteria, the substrate of CusF and its precise role in metal resistance have not been described. Here, isothermal titration calorimetry (ITC) was used to demonstrate that CusF binds with high affinity to both Cu^I and Ag^I but not Cu^{II}. The affinity of CusF for Ag^I was higher than that for Cu^I, which could reflect more efficient detoxification of Ag^I given the lack of a cellular need for Ag^I. The chemical shifts in the nuclear magnetic resonance (NMR) spectra of CusF−Ag^I as compared to apo-CusF show that the region of CusF most affected by Ag^I binding encompasses three absolutely conserved residues: H36, M47, and M49. This suggests that these residues may play a role in Ag^I coordination. The NMR spectra of CusF in the presence of Cu^{II} do not indicate specific binding, which is in agreement with the ITC data. We conclude that Cu^I and Ag^I are the likely physiological substrates.

Metal homeostasis is a crucial function for all organisms. The cellular requirements for a particular metal must be balanced against the toxic effects of an overabundance of that metal. When in excess, metals are exported from cells or detoxified by a variety of mechanisms depending upon the organism, the concentration of the metal, and the metal species (*1*).

Metal homeostasis systems require specificity to address the differing cellular needs and toxicities of different metals. Metal resistance systems are therefore usually specific to a small number of metals with related properties. For example, the Czc resistance system of *Ralstonia metallidurans* is responsible for exporting the divalent ions Co^{II}, Zn^{II}, and Cd^{II} (*2*), while the Mer system of most Gram-negative bacteria detoxifies Hg^{II} and organomercurials (*1*).

Copper and silver have some similar properties and are of particular interest medically and environmentally because of their use as antimicrobial agents. Because of its ability to convert between reduced and oxidized states, copper is used as a cofactor in a number of metalloenzymes that transfer electrons and transport and activate dioxygen. Critical functions, including antioxidant defense and mitochondrial respiration, rely on these metalloenzymes. However, the same redox ability that makes copper a valuable coenzyme also

makes it extremely toxic. Free copper ions will form hydroxyl radicals that can damage cellular components, including proteins, lipids, and nucleic acids (*3−6*). Cellular susceptibility to excessive copper concentrations has led to its use as a biocide in a variety of environmental applications. Silver, unlike copper, does not readily undergo redox transformations and has no known useful function in organisms. However, silver is still toxic because it disrupts both normal enzymatic and membrane function (*7*, *8*). It has been used extensively as a topical antimicrobial agent in newborn eye drops, in bandages for trauma wounds and burns, as well as other applications (*9*).

Perhaps as a consequence of the increased use of copper and silver against microbes, resistance systems, often plasmid-encoded, have emerged in a number of microorganisms (*9−12*). This provides a motivation for the study of systems that regulate cellular levels of these metals, such as the *cus* operon, encoded on the chromosome of *Escherichia coli*. The Cus system has four protein components: CusC, CusF, CusB, and CusA. The CusA component is a member of the RND (resistance, nodulation, and division) transporter family. CusA, together with the outer membrane protein, CusC, and the membrane fusion protein, CusB, is proposed to form a copper-exporting complex spanning both the inner and outer membranes of *E. coli* similar to that of the multidrug exporters such as AcrAB-TolC (*13*). Proteins of this family use the proton gradient to drive the translocation of substrates up a concentration gradient and across the outer membrane (*14*).

CusF homologues are only found in putative copper and silver CBA-type exporter systems and not in the CBA systems that transport drugs and proteins (*13*). CusF has no significant sequence similarity to other characterized proteins,

* To whom correspondence should be addressed: Department of Biochemistry and Molecular Biophysics, 1041 E. Lowell St., University of Arizona, Tucson, AZ 85721. Fax: (520) 621-1697. E-mail: mcevoy@email.arizona.edu.
[‡] Department of Biochemistry and Molecular Biophysics.
[§] Department of Soil, Water, and Environmental Science.

although similar sequences are found in some uncharacterized open-reading frames from other bacteria. The genes encoding these hypothetical proteins are in operons that also encode CusCBA homologues, leading to the suggestion that these proteins may also be involved in metal resistance. CusF may function as a metallochaperone, bringing metal from the periplasm to a channel in the efflux pump to be exported from the cell (*11*, *13*, *15*), or perhaps, CusF may function as a regulator of the CBA channel function. The crystal structure of apo-CusF has recently been reported (*16*). Its fold, which belongs to the OB-fold family, is unlike other copper chaperones, which display folds such as a ferredoxin-like fold [Hah1 (*17*), Atx1 (*18*), and CopZ (*19*)], a thioredoxin-like fold [Sco1 (*20*)], a cupredoxin-like fold [CopC (*21*) and PcoC (*22*)], or a helical hairpin motif [Cox17 (*23*)].

The metal(s) serving as a physiological substrate of CusF has been a matter of some debate. In *E. coli*, the CusCFBA system was originally described as a silver resistance system but was later shown to play a role in copper homeostasis as well (*11*, *13*, *15*, *24*). CusF was initially reported to bind Cu^{II} by inductively coupled plasma mass spectrometry (ICP-MS) (*13*). However, Outten et al. have shown that the *cus* system is more important under anaerobic conditions (*15*), which suggests that the physiological copper species may be Cu^I, which would predominate under such conditions. Cu^I was previously reported to bind CusF but with unknown affinity (*16*). To help elucidate the biochemical role of CusF in the Cus efflux system, isothermal titration calorimetry (ITC)[1] and nuclear magnetic resonance (NMR) spectroscopy were used to determine the specificity, mode of recognition, and binding site of CusF for Cu^I, Cu^{II}, and Ag^I.

MATERIALS AND METHODS

Preparation of CusF for ITC Experiments. E. coli BL21-DE3 cells containing the pASK-IBA3 (IBA, Göttingen, Germany) plasmid with the gene encoding CusF, were grown in LB media. After an OD$_{600}$ of 0.6−1.0 was reached, cells were induced with 200 μg/L anhydrotetracycline. After cells grew for 6−8 h, they were harvested by centrifugation and frozen at −80 °C. Cell pellets were resuspended in approximately 50 mL of 100 mM Tris (pH 8.0) and 150 mM NaCl per liter of cell culture. Cells were lysed using a French press, and the insoluble material was removed by centrifugation (4 °C and 31000g). The soluble fraction was dialyzed versus 60 mM lactate (pH 3.5), which removed a large number of contaminating proteins through precipitation, leaving CusF in solution. After centrifugation at 31000g, the supernatant was loaded onto a HighPrep 16/10 Sepharose Fast Flow (Amersham) ion-exchange column equilibrated with lactate buffer. The column was washed with lactate buffer, and then CusF was eluted from the column with a linear gradient from 100 to 500 mM NaCl in 60 mM lactate (pH 3.5). Samples of each fraction were run on a sodium dodecyl sulfate (SDS)−polyacrylamide gel and stained with Coomassie to determine purity. The CusF-containing fractions were pooled and then concentrated to 1 mL; an equal amount of Milli-Q purified water was added; and the sample was again concentrated to 1 mL to lower the salt concentra-

tion. The sample was then loaded onto a HighPrep Sephacryl S-100 high-resolution (Amersham) gel-filtration column equilibrated with 100 mM sodium phosphate and 100 mM NaCl (pH 7) buffer. The protein was eluted with 250 mL of the phosphate buffer. CusF-containing fractions were pooled, incubated overnight with 1 mM ethylenediaminetetraacetic acid (EDTA), and then dialyzed against Chelex-treated 50 mM *N,N,N'*-trimethylethylenediamine (TMED) at pH 9 with either 30 mM NaCl or 30 mM KNO$_3$ for ITC. From visualization on a Coomassie-stained SDS gel, the final material was judged to be greater than 95% pure. The CusF concentration was determined from a bicinchoninic acid (BCA)-based protein assay (Pierce Biotechnology, Inc.) using the standard protocol as supplied from the manufacturer.

ITC. ITC measurements were performed on a MicroCal VP-ITC microcalorimeter (Northampton, MA). Aerobic titrant solutions were made by mixing appropriate amounts of stock metal solution (1 M metal in nanopure Milli-Q water) with buffer retained from the final dialysis of the protein sample. Anaerobic titrant solutions were prepared by making 20× stock solutions (10 mM metal in nanopure Milli-Q water with 1 M NaCl) inside an anaerobic chamber and then mixing with buffer retained from the final dialysis of the protein sample. Both the sample and titrant solutions were thoroughly degassed before each titration. The reaction cell was stirred at 300 rpm to ensure good mixing. For a typical titration, 1.7 mL of 25 μM CusF solution was injected with 10 μL metal solution over 20 s every 5 min following an initial injection of 2 μL. To measure Ag^I binding, 16 total injections of 0.25 mM AgNO$_3$ were made at 25 °C, using KNO$_3$ in the buffer instead of NaCl to enhance silver solubility. To measure Cu^I binding, 28 total injections of 0.5 mM CuCl were made into the protein solution at 26 °C. Experiments with Cu^I were performed entirely in an anaerobic chamber to ensure the proper oxidation state of the titrant solution over the course of the titration. The heats because of dilution, mechanical effects, and other nonspecific effects were accounted for by averaging the last three points of the titration and subtracting that value from all data points (*25*–*27*). This correction was done because the heats observed for Ag^I titrated into buffer were significantly lower than those observed in the final points of the corresponding experimental titrations, which is likely due to nonspecific interactions of the metal and protein. Control titrations of metal into buffer cannot account for nonspecific binding effects. The control titration for Cu^I exhibited more complex behavior and is discussed in the Results. The first point was removed before analysis to account for anomalies in the first injection because of diffusion from the syringe during equilibration. Each titration was repeated 3 times to ascertain reproducibility. Binding constants and stoichiometries were estimated from the resulting titration curves using either a single set of equivalent sites model or a two noninteracting sets of equivalent sites model in the Origin analysis software (version 5.0, MicroCal, Inc.) (*28*, *29*). The software uses a nonlinear least-squares algorithm and the concentrations of the titrant and the sample to fit the heat developed or consumed in each injection to an equilibrium binding equation. The number of transitions seen in the ITC traces dictated the choice of either a single- or double-site-binding model for curve-fitting.

---

[1] Abbreviations: ITC, isothermal titration calorimetry; NMR, nuclear magnetic resonance; TMED, *N,N,N'*-trimethylethylenediamine.

Preparation of CusF for NMR Experiments. The protocol for the preparation of CusF for the NMR experiments is similar to that described above, except that cells were grown in M9 minimal medium containing [^{15}N]ammonium chloride and [^{13}C]glucose-d_6 as sole nitrogen and carbon sources for isotopic labeling. Cells were grown for 12−14 h after induction. CusF was purified as described above, and comparable purity was achieved. Samples were dialyzed against 50 mM sodium phosphate (pH 7.5) and concentrated to an approximately 1 mM final CusF concentration. Equimolar amounts of CuCl$_2$ and AgNO$_3$ were added for the Cu^{II}−CusF and Ag^{I}−CusF spectra, respectively. A total of 0.02% NaN$_3$ and 10% D$_2$O were added to the samples, which were then placed in NMR tubes.

NMR Data Collection. Spectra were collected at 25 °C on a Varian Inova 600 MHz NMR instrument equipped with a 5 mm triple-resonance, z-axis gradient probe. Fast ^{1}H-^{15}N heteronuclear single-quantum coherence (HSQC) spectra and the HNCA (*30*) spectrum were collected using the standard pulse sequences from Varian BioPack. For CusF−Ag^{I}, backbone resonance assignments were determined by following connectivities in the HNCA spectrum. Spectra were processed with NMRPipe (*31*) and analyzed with NMRView (*32*).

RESULTS

Metal Affinity of CusF Measured by ITC. Because the Cus system is important for copper and silver tolerance in *E. coli*, the thermodynamics of binding of Ag^{I}, Cu^{I}, and Cu^{II} to CusF was determined by ITC. As Ag^{I} was titrated into a solution of CusF, the amount of heat released was measured for each injection (Figure 1). The steep transition in the amount of heat released is characteristic of a single tight binding site. Analysis of the binding isotherm with the Origin software package using a single-site-binding model approximated the dissociation constant to be 38 ± 6 nM. Because this value approaches the lower limit of binding directly measurable by ITC (*33*), it only approximates the exact binding affinity; however, it clearly indicates very strong binding of Ag^{I} to CusF. The data are best fit to a model with a binding stoichiometry of 0.52 ± 0.08 silver ions/CusF molecule. Attempting to force a stoichiometry of 1:1 results in a poor fit of the data ($\chi^2 = 2 \times 10^6$ instead of 8×10^3). The best fit stoichiometry of 0.5 silver ions to one CusF molecule could imply that CusF dimerizes upon Ag^{I} binding. However, a second transition is not observed in the ITC traces, which would indicate a second event such as dimerization, and the linewidths of the NMR spectra (see the following section) do not show broadening in the presence of Ag^{I} that would result from a doubling in the molecular weight. Thus, we conclude that the most likely interpretation is that one silver ion is bound per CusF molecule. If a small amount of trace metal contamination persisted despite the treatment of all buffers with Chelex resin, this could lead to an underestimation of the ratio of silver to CusF. Clearly, though, CusF binds to Ag^{I} very tightly. Table 1 summarizes the binding parameters obtained.

The titration of Cu^{I} into CusF, shown in Figure 2, exhibited more complex behavior involving both exo- and endothermic reactions. Taken alone, this pattern of heat release is usually indicative of two independent binding sites. However, a
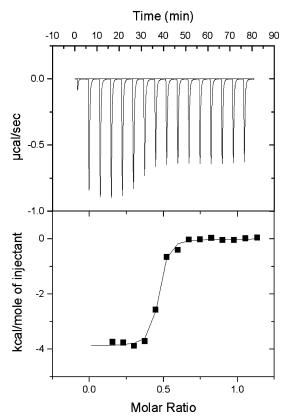

FIGURE 1: Typical ITC data for 0.25 mM AgNO$_3$ titrated into 25 μM CusF at 25 °C. Both solutions were in 50 mM TMED and 30 mM KNO$_3$ at pH 9. The upper panel presents the calorimetric trace, while the bottom panel shows the integrated heats of injection. The solid line represents the best fit for a single-site-binding model. The thermodynamic parameters are listed in Table 1.

Table 1: Binding Affinities for the Binding of Ag^{I} and Cu^{I} to CusF Obtained by ITC Measurements[a]

ligand	binding stoichiometry (n)	association constant, K_a (μM^{-1})	dissociation constant, K_d[b] (nM)
Ag^{I}	0.52 ± 0.08	26.4 ± 3.8	38.5 ± 6.0
Cu^{I}	0.82 ± 0.09	2.72 ± 2	495 ± 260
Cu^{II}	n/a	<0.04[c]	>25 000

[a] All standard deviations were derived from triplicate runs. [b] Values were calculated from experimentally determined parameters. [c] Maximum possible value was calculated from the lowest theoretically measurable association constant using a macromolecular concentration (*M*) of 25 μM, according the rule $K_a M > 1$ (*28*).

control titration of Cu^{I} into buffer exhibited an endothermic binding isotherm qualitatively and quantitatively similar to that seen in the experimental titration, without any exothermic binding behavior (see Figure 1S of the Supporting Information). When a binding event occurs, it is inappropriate to simply subtract those heats from another titration because both events are competing for the same ligand. Accordingly, the experimental isotherms were fit using a two-site-binding model, and only the exothermic binding site, representing Cu^{I} binding to CusF, is reported here. These data show that Cu^{I} binds to CusF with a moderate affinity, with a dissociation constant estimated at 495 ± 260 nM from a best fit of the data (Table 1). The determined stoichiometry of 0.82 ± 0.09 copper ions per CusF molecule is consistent with a single copper-binding site on the protein.

Previous reports indicated the possibility that CusF could bind to Cu^{II} based on ICP-MS (*13*) and electron paramagnetic
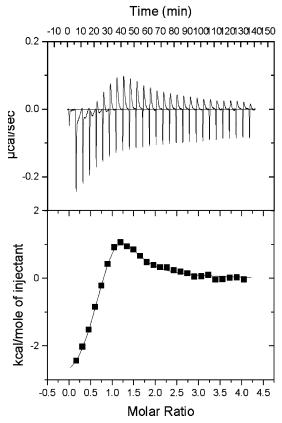
FIGURE 2: Typical ITC data for 0.5 mM CuCl titrated into 25 μM CusF at 26 °C under anaerobic conditions. Both solutions were in 50 mM TMED and 30 mM NaCl at pH 9. The upper panel presents the calorimetric trace, while the bottom panel shows the integrated heats of injection. The solid line represents the best fit for a two-site-binding model. The thermodynamic parameters for the first Cu[I] binding are listed in Table 1.

resonance (EPR) studies (*34*) of an affinity-tagged version of CusF. To test whether the naturally occurring form of CusF with no extraneous modifications could bind to Cu[II], we performed a titration of CusF with Cu[II]. Unlike the results seen in the Cu[I] titration, no significant effects were observed up to a 5-fold molar excess of Cu[II], indicating a lack of specific binding (see Figure 2S in the Supporting Information).

NMR of Metal-Bound CusF. To determine how CusF interacts with Ag[I], we collected ^{1}H^N-^{15}N correlation spectra of CusF bound to Ag[I]. Because resonances are observed from the amide group in the backbone of each amino acid except proline, these experiments provide a sensitive means to simultaneously probe each residue for effects upon the addition of metal.

The binding of Ag[I] by CusF causes numerous changes in the positions of peaks in the ^{1}H^N-^{15}N correlation spectra (Figure 3). No significant line-broadening was observed upon the addition of Ag[I], which implies that a higher molecular-weight species such as a dimer is not formed in the complex. To determine the magnitude of the spectral changes, we assigned the backbone ^{1}H^N, ^{15}N, and C$^\alpha$ resonances of CusF–Ag[I] using a through-bond correlation experiment. Chemical-shift changes upon the addition of Ag[I] were plotted in Figure 4 as the weighted average ^{1}H^N-^{15}N chemical shift as given by $\Delta_{av} = [(\Delta\delta_{NH}^2 + \Delta\delta_N^2/25)/2]^{1/2}$. The most significant changes (greater than 0.16 ppm) because of the addition of Ag[I] were seen for residues M47, T48, R50, D37, H36, W44,
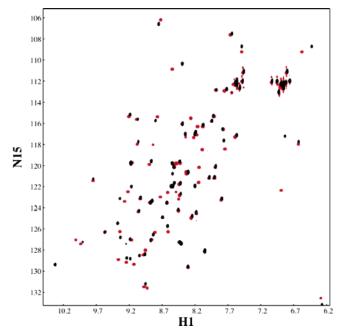

FIGURE 3: ^{1}H^N-^{15}N correlation spectra of CusF–Ag[I] (black) and apo-CusF (red).

M8, A40, E46, Q75, and H35. These residues are clustered in CusF at one end of the β barrel (inset of Figure 4).

In contrast, when Cu[II] was added to the protein, no significant shift changes were observed beyond the disappearance of peaks representing residues close to the N terminus (Figure 5). Because Cu[II] is paramagnetic, peaks that are in close proximity to Cu[II] are expected to broaden and thus disappear from the spectrum. When Cu[II] is added to CusF, three peaks disappear and another three weaken. Most of these residues are close to the N terminus: the resonances of residues 6–8 disappear and that of residue 9 weakens. Residues 1–5 have not been assigned in any spectra of CusF; however, their identity is NEHHH. The presence of these histidine side chains could lead to weak binding of Cu[II] at that site and thus cause broadening of residues 6–9 because of the close proximity to the paramagnetic metal species.

DISCUSSION

CusF may play a role as a metallochaperone in the Cus system and may be involved in conferring some specificity for the transported species. Previous work suggested that the Cus system was important for cellular resistance to Ag[I] (*24*), Cu[I] (*15*), and possibly Cu[II] (*13*). To determine whether CusF could specifically bind these ions and to describe their binding sites, we undertook ITC and NMR studies.

Titration of CusF with Cu[II], as observed by ITC, shows no indication of specific binding. The addition of Cu[II] to apo-CusF causes the loss and broadening of several NMR peaks, primarily in the N-terminal region near where three consecutive histidines are located. However, this is likely a consequence of weak or nonspecific binding to the His-rich region at the N terminus and is observed only because of the high concentrations of both protein and Cu[II] present in the NMR sample. From these experiments, we conclude that Cu[II] does not specifically and tightly bind to CusF and thus is not likely to be a physiological substrate.

The ITC and NMR experiments with CusF and Ag[I] indicate that Ag[I] binds tightly and specifically to CusF. The
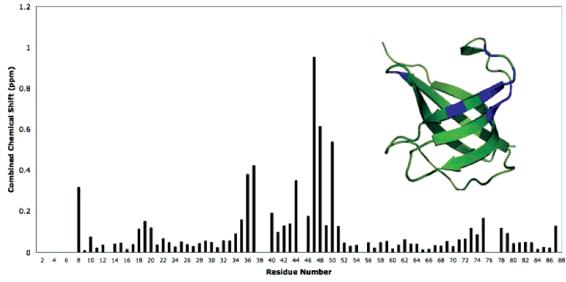
FIGURE 4: Combined $^1H^N$-^{15}N chemical-shift changes as a function of the residue number of CusF−Ag^I. The absolute value of the chemical-shift change for the metal-bound CusF relative to apo-CusF is reported. (Inset) Ribbon diagram of apo-CusF showing residues 11−88 [PDB 1ZEQ (*16*)] Residues with chemical shifts significantly affected by Ag^I binding are colored blue.
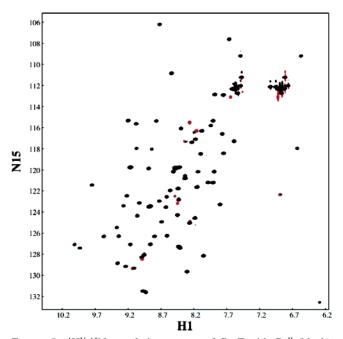

FIGURE 5: $^1H^N$-^{15}N correlation spectra of CusF with Cu^{II} (black) and apo-CusF (red).

single sharp transition seen in the ITC titration of CusF with Ag^I confirms that CusF specifically binds Ag^I. The NMR spectrum of CusF−Ag^I shows a single species with sharp linewidths, which also indicates specific binding. In CusF, Ag^I is bound about 1 order of magnitude more tightly than Cu^I (38 and 495 nM, respectively). The source for this difference may be attributed to the strong preference of silver ions for sulfur ligands (*2*). The two ions have different effective ionic radii, which are approximately 0.46−0.60 and 0.67−1.00 Å, respectively, for Cu^I and Ag^I for coordination numbers from two to four (*35*). The size differential may also contribute to the differing affinities. However, multiple factors contribute to binding affinities in copper- and silver-binding proteins; therefore, one ion is not always preferred (*36, 37*).

Assuming that the binding affinities of CusF are representative of the substrate preferences of the CusCFBA system, the differential binding affinities for Cu^I and Ag^I are consistent with the biological needs of *E. coli*. While there are no known enzymes that require Ag^I for proper function, several *E. coli* enzymes found in the periplasm do need Cu^I as a cofactor (*11*). Thus, extruding Ag^I with high efficiency has no negative impact on the cell, while export of the entire Cu^I pool could potentially deprive enzymes of a needed metal ion.

The NMR spectrum of CusF−Ag^I shows similar chemical-shift changes to those previously reported by us for CusF−Cu^I (*16*). On the basis of absolute sequence conservation among homologues, proximity in the structure, and significant NMR chemical-shift changes upon Cu^I addition, Cu^I was proposed to be coordinated in a trigonal planar geometry by CusF residues M47, M49, and H36 (*16*). The chemical-shift changes observed in the NMR spectra upon the addition of Ag^I suggest that these residues may be involved in Ag^I binding as well. Because they share similar d^{10} valence configurations, Cu^I and Ag^I are generally capable of the same coordination chemistry (*38*). For example, CueR has been reported to bind both ions with a linear two-coordinate geometry using the same ligands (*39*). However, the two ions do not necessarily behave the same in all cases (*40*). For example, in hemocyanin, Ag^I takes an extra water ligand as compared to Cu^I, and Cox17, the copper chaperone for cytochrome *c* oxidase, binds Cu^I with high affinity but does not bind Ag^I at all (*41, 42*). In the case of Cox17, which has a multinucleate CuS cluster, the authors suggest that the preference for a particular ion may be due to the size difference between copper and silver.

In only one other case has the affinity for Cu^I been determined for a periplasmic metal-binding protein. CopC, a periplasmic copper carrier protein from *Pseudomonas syringae*, is proposed to bind Cu^I using histidine and methionine residues (*21, 43*), with a K_d in the range from 10^{-7} to 10^{-13} M (*44*). Thus, the weaker binding limit of CopC is similar to the measured affinity of CusF for Cu^I. CopC is different from CusF in that it has separate high-affinity binding sites for both Cu^I and Cu^{II} (*43, 44*). The affinity of CopC for Ag^I has not been reported.

The structure of a cytoplasmic protein, CueR, involved in the regulation of metal-responsive genes has been determined in the Cu^I, Ag^I, and Au^I states (*39*). In all cases, the monovalent cations are similarly coordinated by two cysteine residues. The affinity of CueR for Cu^I has been reported to be in the zeptomolar range (*39*), but the affinity for Ag^I has not been determined. CueR may have an exceedingly high affinity for Cu^I because of its location in the cytoplasm where Cu^I concentrations are expected to be extremely low. In the periplasm, where free copper concentrations may be greater, very high affinity may not be required to prevent toxic effects of excess free copper.

The magnitude of the combined chemical-shift changes for the backbone amides is slightly different for Ag^I and Cu^I, particularly for residues T48 and M49. These residues, along with M47, show the largest chemical-shift changes upon Cu^I binding (*16*). Although M47 is still affected by the binding of Ag^I, T48 and M49 show a chemical-shift change of only about $^1/_4$ of that upon Cu^I binding. Decreased chemical-shift changes for M49 may indicate that Ag^I might only be coordinated by two residues: H36 and M47. However, magnitude differences are difficult to interpret because many factors contribute to chemical-shift changes. Chemical-shift changes are reflective of perturbations in the local electronic environment but do not necessarily reflect a direct involvement in interactions. Overall, because the general trend of chemical-shift changes is similar with both ions, it is likely that Ag^I binds in the same site as Cu^I in CusF and is causing the same global effect on the protein.

The chemical-shift changes localized at one of the β barrel of CusF may indicate a metal-induced conformational change that could facilitate the transfer of metal to the efflux complex. Alternatively, CusF may be a metal-activated regulator that stimulates the export activity of the efflux complex. Now that we have defined the biochemical properties of CusF, future studies will be directed toward understanding how this fits in with the activity of the entire export apparatus.

SUPPORTING INFORMATION AVAILABLE

ITC data of buffer titrated with Cu^I (Figure 1S) and CusF titrated with Cu^{II} (Figure 2S). This material is available free of charge via the Internet at http://pubs.acs.org.

REFERENCES

1. Silver, S., and Phung, L. T. (2005) A bacterial view of the periodic table: Genes and proteins for toxic inorganic ions, *J. Ind. Microbiol. Biotechnol. 32*, 587−605.

2. Nies, D. H. (2003) Efflux-mediated heavy metal resistance in prokaryotes, *FEMS Microbiol. Rev. 27*, 313−339.

3. Ramirez, D. C., Mejiba, S. E., and Mason, R. P. (2005) Copper-catalyzed protein oxidation and its modulation by carbon dioxide: Enhancement of protein radicals in cells, *J. Biol. Chem. 280*, 27402−27411.

4. Bertinato, J., and L'Abbe, M. R. (2004) Maintaining copper homeostasis: Regulation of copper-trafficking proteins in response to copper deficiency or overload, *J. Nutr. Biochem. 15*, 316−322.

5. Valko, M., Morris, H., and Cronin, M. T. (2005) Metals, toxicity and oxidative stress, *Curr. Med. Chem. 12*, 1161−1208.

6. Stohs, S. J., and Bagchi, D. (1995) Oxidative mechanisms in the toxicity of metal ions, *Free Radical Biol. Med. 18*, 321−336.

7. Percival, S. L., Bowler, P. G., and Russell, D. (2005) Bacterial resistance to silver in wound care, *J. Hosp. Infect. 60*, 1−7.

8. Silver, S., Phung L. T., and Silver, G. (2006) Silver as biocides in burn and wound dressings and bacterial resistance to silver compounds, *J. Ind. Microbiol. Biotechnol. 33*, 627−634.

9. Silver, S. (2003) Bacterial silver resistance: Molecular biology and uses and misuses of silver compounds, *FEMS Microbiol. Rev. 27*, 341−353.

10. Hendry, A. T., and Stewart, I. O. (1979) Silver-resistant enterobacteriaceae from hospital patients, *Can. J. Microbiol. 25*, 915−921.

11. Rensing, C., and Grass, G. (2003) *Escherichia coli* mechanisms of copper homeostasis in a changing environment, *FEMS Microbiol. Rev. 27*, 197−213.

12. Voloudakis, A. E., Reignier, T. M., and Cooksey, D. A. (2005) Regulation of resistance to copper in *Xanthomonas axonopodis* pv. *vesicatoria*, *Appl. Environ. Microbiol. 71*, 782−789.

13. Franke, S., Grass, G., Rensing, C., and Nies, D. H. (2003) Molecular analysis of the copper-transporting efflux system CusCFBA of *Escherichia coli*, *J. Bacteriol. 185*, 3804−3812.

14. Tseng, T. T., Gratwick, K. S., Kollman, J., Park, D., Nies, D. H., Goffeau, A., and Saier, M. H., Jr. (1999) The RND permease superfamily: An ancient, ubiquitous and diverse family that includes human disease and development proteins, *J. Mol. Microbiol. Biotechnol. 1*, 107−125.

15. Outten, F. W., Huffman, D. L., Hale, J. A., and O'Halloran, T. V. (2001) The independent *cue* and *cus* systems confer copper tolerance during aerobic and anaerobic growth in *Escherichia coli*, *J Biol. Chem. 276*, 30670−30677.

16. Loftin, I. R., Franke, S., Roberts, S. A., Weichsel, A., Heroux, A., Montfort, W. R., Rensing, C., and McEvoy, M. M. (2005) A novel copper-binding fold for the periplasmic copper resistance protein CusF, *Biochemistry 44*, 10533−10540.

17. Anastassopoulou, I., Banci, L., Bertini, I., Cantini, F., Katsari, E., and Rosato, A. (2004) Solution structure of the apo and copper-(I)-loaded human metallochaperone HAH1, *Biochemistry 43*, 13046−13053.

18. Arnesano, F., Banci, L., Bertini, I., Huffman, D. L., and O'Halloran, T. V. (2001) Solution structure of the Cu(I) and apo forms of the yeast metallochaperone, Atx1, *Biochemistry 40*, 1528−1539.

19. Banci, L., Bertini, I., Del Conte, R., Markey, J., and Ruiz-Duenas, F. J. (2001) Copper trafficking: The solution structure of *Bacillus subtilis* CopZ, *Biochemistry 40*, 15660−15668.

20. Balatri, E., Banci, L., Bertini, I., Cantini, F., and Ciofi-Baffoni, S. (2003) Solution structure of Sco1: A thioredoxin-like protein involved in cytochrome *c* oxidase assembly, *Structure 11*, 1431−1443.

21. Arnesano, F., Banci, L., Bertini, I., and Thompsett, A. R. (2002) Solution structure of CopC: A cupredoxin-like protein involved in copper homeostasis, *Structure 10*, 1337−1347.

22. Wernimont, A. K., Huffman, D. L., Finney, L. A., Demeler, B., O'Halloran, T. V., and Rosenzweig, A. C. (2003) Crystal structure and dimerization equilibria of PcoC, a methionine-rich copper resistance protein from *Escherichia coli*, *J. Biol. Inorg. Chem. 8*, 185−194.

23. Abajian, C., Yatsunyk, L. A., Ramirez, B. E., and Rosenzweig, A. C. (2004) Yeast Cox17 solution structure and copper(I) binding, *J. Biol. Chem. 279*, 53584−53592.

24. Franke, S., Grass, G., and Nies, D. H. (2001) The product of the *ybdE* gene of the *Escherichia coli* chromosome is involved in detoxification of silver ions, *Microbiology 147*, 965−972.

25. Jelesarov, I., and Bosshard, H. R. (1999) Isothermal titration calorimetry and differential scanning calorimetry as complementary tools to investigate the energetics of biomolecular recognition, *J. Mol. Recognit. 12*, 3−18.

26. Leavitt, S., and Freire, E. (2001) Direct measurement of protein binding energetics by isothermal titration calorimetry, *Curr. Opin. Struct. Biol. 11*, 560−566.

27. Kaspar, S., Perozzo, R., Reinelt, S., Meyer, M., Pfister, K., Scapozza, L., and Bott, M. (1999) The periplasmic domain of the histidine autokinase CitA functions as a highly specific citrate receptor, *Mol. Microbiol. 33*, 858−872.

28. Wiseman, T., Williston, S., Brandts, J. F., and Lin, L. N. (1989) Rapid measurement of binding constants and heats of binding using a new titration calorimeter, *Anal. Biochem. 179*, 131−137.

29. Indyk, L., and Fisher, H. F. (1998) Theoretical aspects of isothermal titration calorimetry, *Energ. Biol. Macromol., Part B 295*, 350−364.

30. Bax, A., and Ikura, M. (1991) An efficient 3D NMR technique for correlating the proton and ^{15}N backbone amide resonances with the α-carbon of the preceding residue in uniformly ^{15}N/^{13}C enriched proteins, *J. Biomol. NMR 1*, 99−104.

31. Delaglio, F., Grzesiek, S., Vuister, G. W., Zhu, G., Pfeifer, J., and Bax, A. (1995) NMRPipe: A multidimensional spectral processing system based on UNIX pipes, *J. Biomol. NMR 6*, 277−293.

32. Johnson, B. A., and Blevins, R. A. (1994) NMRView: A computer program for the visualization and analysis of NMR data, *J. Biomol. NMR 4*, 603−614.

33. Velazquez Campoy, A., and Freire, E. (2005) ITC in the post-genomic era? Priceless, *Biophys. Chem. 115*, 115−124.

34. Astashkin, A. V., Raitsimring, A. M., Walker, F. A., Rensing, C., and McEvoy, M. M. (2005) Characterization of the copper(II) binding site in the pink copper binding protein CusF by electron paramagnetic resonance spectroscopy, *J. Biol. Inorg. Chem. 10*, 221−230.

35. Shannon, R. D. (1976) Revised effective ionic-radii and systematic studies of interatomic distances in halides and chalcogenides, *Acta Crystallogr., Sect. A: Found. Crystallogr. 32*, 751−767.

36. Hay, M. T., and Lu, Y. (2000) Metal-binding properties of an engineered purple Cu-A center in azurin, *J. Biol. Inorg. Chem. 5*, 699−712.

37. Mandal, A. K., Cheung, W. D., and Arguello, J. M. (2002) Characterization of a thermophilic P-type Ag$^+$/Cu$^+$-ATPase from the extremophile *Archaeoglobus fulgidus*, *J. Biol. Chem. 277*, 7201−7208.

38. Gitschier, J., Moffat, B., Reilly, D., Wood, W. I., and Fairbrother, W. J. (1998) Solution structure of the fourth metal-binding domain from the Menkes copper-transporting ATPase, *Nat. Struct. Biol. 5*, 47−54.

39. Changela, A., Chen, K., Xue, Y., Holschen, J., Outten, C. E., O'Halloran, T. V., and Mondragon, A. (2003) Molecular basis of metal-ion selectivity and zeptomolar sensitivity by CueR, *Science 301*, 1383−1387.

40. Palacios, O., Polec-Pawlak, K., Lobinski, R., Capdevila, M., and Gonzalez-Duarte, P. (2003) Is Ag(I) an adequate probe for Cu(I) in structural copper-metallothionein studies? The binding features of Ag(I) to mammalian metallothionein 1, *J. Biol. Inorg. Chem. 8*, 831−842.

41. Holm, J. K., Hemmingsen, L., Bubacco, L., Salvato, B., and Bauer, R. (2000) Interaction and coordination geometries for Ag(I) in the two metal sites of hemocyanin, *Eur. J. Biochem. 267*, 1754−1760.

42. Palumaa, P., Kangur, L., Voronova, A., and Sillard, R. (2004) Metal-binding mechanism of Cox17, a copper chaperone for cytochrome *c* oxidase, *Biochem. J. 382*, 307−314.

43. Arnesano, F., Banci, L., Bertini, I., Mangani, S., and Thompsett, A. R. (2003) A redox switch in CopC: An intriguing copper trafficking protein that binds copper(I) and copper(II) at different sites, *Proc. Natl. Acad. Sci. U.S.A. 100*, 3814−3819.

44. Zhang, L., Koay, M., Maher, M. J., Xiao, Z., and Wedd, A. G. (2006) Intermolecular transfer of copper ions from the CopC protein of *Pseudomonas syringae*. Crystal structures of fully loaded Cu(I)Cu(II) forms, *J. Am. Chem. Soc. 128*, 5834−5850.